*Proceedings of Building Simulation 2011:*
*12th Conference of International Building Performance Simulation Association, Sydney, 14-16 November.*

# INTEGRATED DYNAMIC ELECTRIC AND THERMAL SIMULATIONS FOR A RESIDENTIAL NEIGHBORHOOD: SENSITIVITY TO TIME RESOLUTION OF BOUNDARY CONDITIONS

Ruben Baetens[1], Roel De Coninck[2, 3], Lieve Helsen[2] and Dirk Saelens[1]
[1]Building Physics Section, Department of Civil Engineering,
[2]Applied Mechanics and Energy Conversion Section, Department of Mechanical Engineering,
[1,2]K.U.Leuven, BE-3000 Leuven, Belgium
[3]3E, BE-1000 Brussels, Belgium

## ABSTRACT

The sensitivity to time resolution of boundary conditions is studied for dynamic integrated simulation of thermal and electrical networks of a net zero energy residential neighborhood. Main energy demands originate from domestic electricity consumption of appliances and an electricity driven heat pump for space heating and domestic hot water production, whereas local energy supply is provided by building integrated photovoltaic (BIPV) systems.

Large simultaneity of net power supply at building level within a residential district results in strong underestimation of grid over-voltages for hourly irradiance data. The use of minutely meteorological data is critical for assessment of power losses due to inverter switch-offs caused by grid voltage increases. On the demand side, the main deviation is found in a possible correlation of heat pump power demands for SH or DHW but not in the stochastic nature of domestic electricity consumption. Here, sub-hourly demand profiles are less critical if they are not used in grid balancing control strategies at building level.

## INTRODUCTION

With a recent European recast 2010/31/EU obliging to build nearly-zero energy buildings (nZEBs) by 2020 (The European Parliament, 2010) and the recent communications of the European Commission on the deployment of a European Smart Grid (European Commission, 2010), a first step is made towards an integrated approach to tackle climate change while still meeting all requests of energy services. Generally, nZEBs face a problem of non-simultaneity between local energy demand and supply. As such, large scale implementation of renewable electricity generation in general and nZEBs in particular will require well developed solutions in the form of energy storage, demand side management or both. As such, the planned developments of smart grids and appropriate control strategies have to be considered as a necessity for integrated optimization.

Simulation-based assessment of the stated problem of non-simultaneity requires an integrated multi-domain approach. Such model is developed in the K.U.Leuven Energy Institute in Modelica (Baetens and Saelens, 2011; De Coninck et al., 2010; Verbruggen et al., 2011) as in fig.1 consisting of the dynamic thermal building response, the dynamics of the domestic hydronic heating system, stochastic user behavior and local energy supply by means of building integrated photovoltaic (BIPV) systems in each dwelling, as well as the low voltage electricity distribution grid between the dwellings. The proposed model differs from existing district models presented in the literature (Heiple and Sailor, 2008; Robinson et al., 2007; Tanimoto et al., 2008; Widén, 2009; Yamaguchi and Shimoda, 2010) by combining the dynamics of the hydronic, thermal as well as electric networks at both the building and district level.

Within this work, a simulation model dealing with the grid interaction of residential buildings is set up. The sensitivity of the model is analyzed for variations in time resolution of the applied boundary conditions, i.e. residential user behavior and meteorological data influencing the local electricity supply by means of BIPVs. Three main reasons may be found for the proposed research from a simulation point of view: First, electricity networks have a much faster response of electricity networks compared to thermal apsects in the built environment which makes electrical measures much more sensitive to time resolution as common building simulations. Second, the sensitivity gives a first indication of the equivalence of different assumptions in simulations especially related to distributed generation and energy balancing at building district level. Last, the implemented detail strongly influences the amount and detail of required knowledge on boundary conditions, and the resulting CPU time for dynamic simulation.

In depth comparison allows to formulate an acceptable level of required detail and knowledge for the boundary conditions of dynamic simulations.

## METHODOLOGY

An integrated energy system model for dynamic simulation of a small residential neighborhood of 33 dwellings is set up. Herefore, an object-oriented approach based on detailed bottom-up modeling of lo-

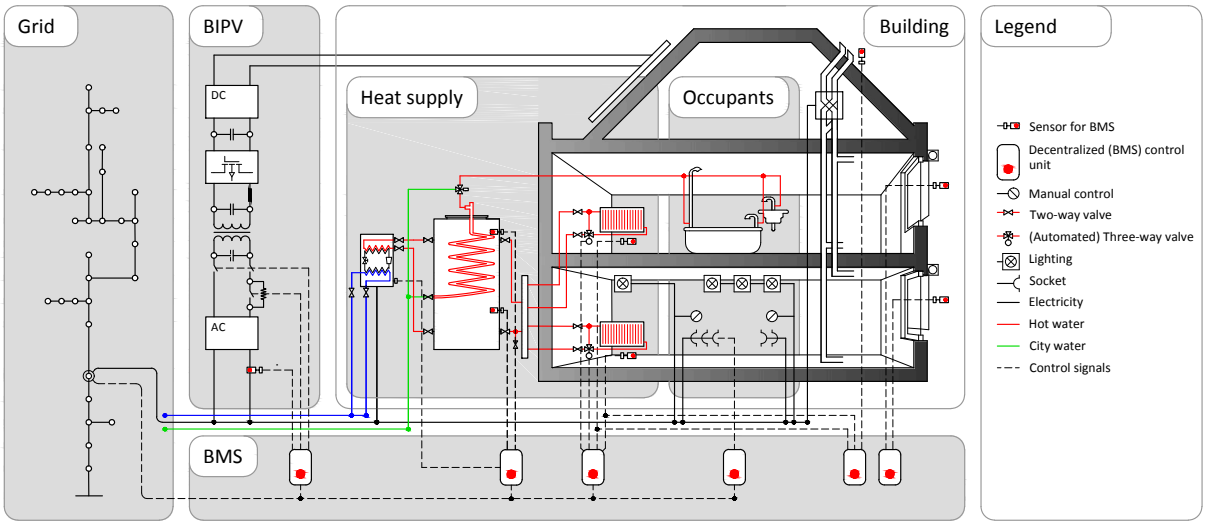


*Figure 1: Representation of the model for integrated dynamic simulation of thermal and electrical energy networks at feeder level. The model includes local electricity generation by means of building integrated photovoltaic (BIPV) systems, stochastic occupant behavior, the thermal building response, the transient behavior of the heating, ventilation and air conditioning system, the building management system (BMS) and the transient response of the low-voltage electrical distribution grid for a residential neighborhood of 33 dwellings.*

cal energy demand and supply has been chosen. This model is simulated using identical parameters but for different time sampling resolution of meteorological data and user behavior. The result is a series of simulations of a small district with equal annual electricity and heat demand and production but showing different results based on the applied detail in boundary conditions. The sensitivity analysis for time resolution of boundary conditions is carried out towards both electrical grid and thermal building performances.

Successively, the residential buildings, their thermal network for space heating (SH) as well as domestic hot water (DHW), and the electrical distribution network are described.

### Residential buildings

Four different detached dwellings as shown in fig.2 are implemented in the district model. The depicted architectural types of the dwellings are determined as representative for the Belgian building stock, and are used in the model based on their statistical spread (Vanneste et al., 2001). With 2010/31/EU (The European Parliament, 2010) in mind, all dwellings are modeled according to a low-energy standard as summarized in table 1, and as 2-zone (i.e. day and night zone) dwellings for dynamic simulation[1]. Although only 4 different physical building models are implemented, all dwellings will show different results during simulation because of the stochastic user behavior defining the internal gains and the required comfort as explained in Ch..

[1]Implementation of the dynamic building model is shortly described in (Baetens and Saelens, 2011). Validation of the model according to ISO 13790 to 13792, and EN 15255 to 15265 is ongoing.

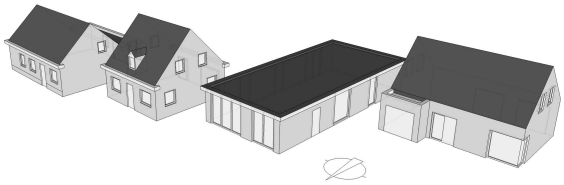

*Figure 2: Representation of the four architectural types of the implemented dwellings.*

All dwellings have an infiltration rate of 0.03 $h^{-1}$ and mechanically balanced, air-to-air heat-recovery ventilation (HRV) with an air change rate of 0.5 $h^{-1}$ and a recovery efficiency of 0.84 $(-)$. To achieve thermal comfort in summer conditions, the HRV unit is bypassed when the temperature of the day-zone surpasses 24°$C$ and is used again when the temperature drops below 19°$C$. It is supposed that occupants open windows when the indoor temperature rises above 24°$C$ resulting in a natural ventilation rate between 3 and 5 $h^{-1}$ depending on the available window sizes. Windows are closed again when the indoor temperature drops below 21°$C$. Summer comfort is further improved by simulating automated exterior shading by means of a solar screen with a short-wave transmittance of 0.24 $(-)$ which is lowered at an irradiance level of 250 $W/m^2$ and raised again below 150 $W/m^2$.

### Hydronic heating systems

Each dwelling has a SH and DHW system with identical configuration, consisting of a modulating air-to-water heat pump (HP), a thermal storage tank, a DHW temperature mixing valve and two radiators, i.e. one for each building zone as visualized in fig.2. The configuration differs for each dwelling on two aspects, i.e.

*Table 1: Summary of the physical properties for the implemented dwellings representative for the four depicted periods.*

| | -'45 | -'70 | -'90 | -'07 |
|---|---|---|---|---|
| Heated area, $m^2$ | 127 | 98 | 149 | 123 |
| Window-floor ratio, $-$ | 0.12 | 0.19 | 0.16 | 0.13 |
| Compactness, $m$ | 1.23 | 1.10 | 0.87 | 1.18 |
| Infiltration rate $n$, $h^{-1}$ | 0.03 | 0.03 | 0.03 | 0.03 |
| $U_{avg}$, $W/(m^2K)$ | 0.145 | 0.174 | 0.159 | 0.158 |
| HRV efficiency $\eta$, $-$ | 0.84 | 0.84 | 0.84 | 0.84 |
| Heat load, $W/m^2$ | 20.5 | 28.0 | 21.6 | 25.9 |

the nominal power of both the heat emission and production devices are adapted to the dwelling's design heat demand (EN 12831, 2003).

The heat pump heats water in a storage tank of 0.25 $m^3$. The model of the storage tank assumes five stratification layers with a uniform temperature and accounts heat exchange between the layers. Two temperature sensors are available in the tank for control purposes, i.e. $T_{top}$ and $T_{bot}$ in the upper and 4th layer respectively. Furthermore, heat losses of the insulated tank to the surroundings are taken into account by an overall heat transfer coefficient of 0.4 $W/(m^2K)$. The storage tank provides hot water for both SH and DHW. The water in the storage tank is used for space heating with low-temperature radiators (i.e. a design inlet and outlet temperature of 55°$C$ and 45°$C$ respectively at a design outdoor temperature of -8°$C$). To simulate, the dynamic behavior of the radiator is a simplified model with a single mixing volume, a dry mass to represent the thermal inertia of steel and a heat transfer coefficient based on the radiator exponent as outlined in EN 442-2 (EN 442-2, 1996). The emission power is modeled with a fixed radiative fraction of 0.30. The DHW is supplied by a heat exchanger in the heating water in the storage tank. A controlled mixing valve sets the output temperature to the set temperature of 45°$C$ while the heat exchanger effectiveness is assumed to be unity.

The heat pump model is based on interpolation in a performance map retrieved from manufacturer data (Daikin Europe N.V., 2006) and a first order dynamic model for the condenser water temperature to account for the capacity and corresponding time constant of the water. The interpolation defines the heating power and electricity use as a function of condenser outlet temperature, the ambient temperature and the modulation within a range of $[0.3, 1.0]$. The coefficient of performance of the heat pump based on manufacturer data (Daikin Europe N.V., 2006) is 3.17 at 2/35°$C$ test conditions (i.e. air/water temperature) and 2.44 at 2/45°$C$ test conditions for full load operation.

The heat pump is controlled by the BMS based on the measured and setpoint values for the storage tank temperatures $T_{top}$ and $T_{bot}$. The setpoints are based on a heating curve for SH and the required temperature for DHW of 45°$C$ which is almost always higher than this heating curve value. The heat pump will be started when $T_{top}$ is 3°$C$ below setpoint and stopped when $T_{bot}$ is 3°$C$ above setpoint. In order to be able to reach the switch off condition on $T_{bot}$, the condenser water set temperature is always 5°$C$ higher than the setpoint. On the heat emission side, on/off controllers are implemented based on the difference between the room setpoint temperature given by the user occupancy, i.e.21°$C$ when occupants are present and 16°$C$ otherwise, and the room operative temperature.

**Domestic hot water**

For domestic hot water (DHW) consumption, the Becker profile (Becker and Stogsdill, 1990) resulting from large scale measurements is chosen based on a comparative literature study (Fairey and Parker, 2004). The profile is a statistical profile averaging the behavior of different users to a single profile, whereas profiles for individual dwellings may be found more peaked.

The DHW production is modeled with an ideal eat exchanger effectiveness between the heating water in the storage tank and the consumed water. A controlled mixing valve sets the output temperature to the set temperature of 45°$C$.

**Electrical distribution grid**

The electricity feeder in the residential district has the same topology as the radial distribution IEEE 34 node test feeder (The Institute of Electrical and Electronics Engineers, 2010) as shwon in fig.2. Since the voltage of the feeder is downscaled to a nominal voltage of 230/400 $V$ wye connected, all line impedances are adapted to obtain a realistic 3-phase low-voltage electricity feeder as described earlier (Verbruggen et al., 2011). The feeder is modeled with cross sections for Aluminum cables of 95, 50 and 35 $mm^2$ with cable lengths of 16 to 48 $m$ between the dwellings as typical for a residential district with detached houses.

Simulations are performed using a single-phase representation of the electrical distribution feeder. The characteristic impedance of the cables is adjusted to represent a 3-phase feeder with symmetrical load.

## RESOLUTION-SENSITIVE BOUNDARY CONDITIONS

In the following paragraph, the factors to which the sensitivity of time resolution is investigated are described, i.e. user behavior and distributed generation.

**Occupant behavior**

Implementation of occupant behavior is described earlier (Baetens and Saelens, 2011). The behavior considering occupancy, the use of lighting and the use of appliances in dwellings is implemented based on

Markov-chains and is consistent with the model of Richardson et al. (Richardson et al., 2010). Bottom-up data concerning household size and installed appliances are determined based on Belgian (FOD Economie, 2008) and European (Richardson et al., 2010) statistics on household sizes and appliance ownership rates respectively. Based on these data, the outputs of the model are: presence and activity of the building occupants determining the required thermal comfort and the use of electric appliances and lighting resulting in internal heat gains and the real electric power demand. As such, the occupant behavior influences both the thermal response of buildings and its grid impact towards the assessment of distributed generation at feeder level.

The original output of the stochastic user profile has a time resolution of 1 minute. Less detailed boundary conditions with a resolution of 5, 10, 15, 30 and 60 minutes respectively are retrieved as time-arithmetic means of the most detailed data.

**Distributed generation**

Implementation of the BIPV system in Modelica is described earlier (Verbruggen et al., 2011). For local electricity supply by means of BIPV systems, irradiance data with a time resolution of 1 minute are obtained artificially using Meteonorm v6.1 for the moderate climate of Uccle (Belgium) and the time period 1981-2000 based on the Skatveith-Olseth model for diffuse radiation (Meteotest, 2008). Less detailed solar irradiation levels with a resolution of 5, 10, 15, 30 and 60 minutes respectively are retrieved as time-arithmetic means of the *Meteonorm* data in order to obtain equivalent profiles.

Sizing of all BIPV systems is based on the total annual electricity consumption for each dwelling to achieve a predicted level of net ZEB. For this theoretical study, all BIPV systems are modeled to be oriented South with an inclination of 34 degrees resulting in the highest annual production.

Due to the resistive character of the feeder, excessive local power supply results in an increased feeder voltage. To avoid excessive voltages, the BIPV system inverter is curtailed when the voltage at the dwellings feeder interface reaches a predefined voltage limit. This limit is set at 110 % of the feeder voltage according to IEC 60364-6 (IEC 60364-6, 2006). The inverter control is given a minimal off-time of 5 $min$ before trying to switch on again after voltage disturbances.

## GENERAL MODEL RESULTS

The resulting winter and summer comfort is represented in fig.3, which shows that the hydronic installations in all dwellings are able to cope with the requested thermal comfort of 21°$C$ during presence and 16°$C$ for absence, and that no zone in all 33 low-energy dwellings show excessive overheating in summer.

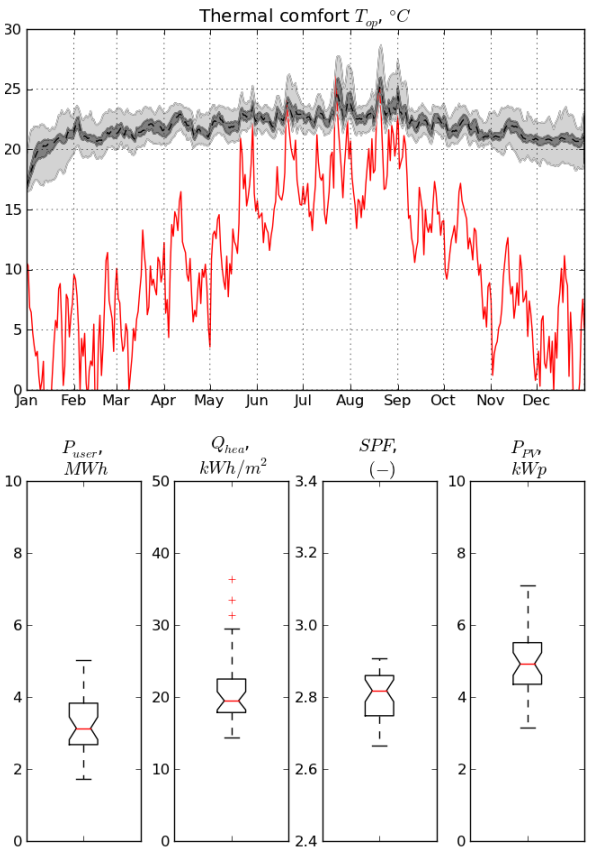


*Figure 3: (upper) Median, lower quartile and upper quartile of the daily average, and min/max extrema of the operative zone temperatures $T_{op}$, and (lower) Tukey-boxplot deviations of the annual domestic electricity consumption $P_{user}$, heat demand $Q_{hea}$ for SH and DHW, the SPF of the HP and the required BIPV capacities $P_{PV}$ to reach a design level of net ZEB for all dwellings.*

For the dwellings in the small district, the household electricity consumption for electric appliances and lighting has a lower and upper quartile of 3.3 ± 0.5 $MWh$, with extrema of 1.8 and 5.2 $MWh$ and is consistent with Belgian statistics (Maes, 2005). The resulting heat demand for SH and DHW defined after dynamic simulation is found to be 18.6 ± 2.5 $kWh/m^2$, with extrema of 14.2 and 36.4 $kWh/m^2$ as show in fig.3, whereas the seasonal performance factor (SPF) of the hydronic installations is found to lie between 2.7 and 2.9. As such, within the moderate climate of Uccle (Belgium), the resulting BIPV capacities to reach a nZEB level at annual basis are 4.9 ± 0.6 kWp, with extrema of 2.2 and 7.1 kWp as shown in fig.3.

## SENSITIVITY TO TIME RESOLUTION

Comparison of the results for each time resolution $G$ is performed based on the histogram for retrieved variables, the deviation of the momentarily deviation $\Delta$

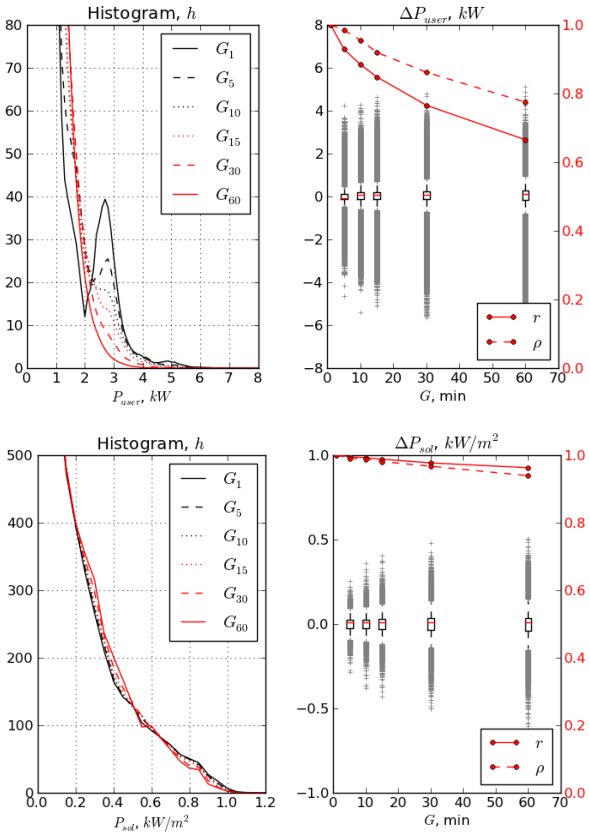


*Figure 4: (right) Deviations as Tukey-boxplot of the momentarily absolute error $\Delta$ in time and the Pearson's product-moment and Spearman's rank correlation coefficients $r$, $\rho$ for the different implemented time resolutions $G$ compared to the most-detailed resolution $G_1$ with 1-minute data, and (left) the overall density curve for the resulting power demand and/or internal heat gain $P_{user}$ due to occupant behavior (upper) and the total solar irradiation $P_{sol}$ on a horizontal surface (lower) respectively.*

of the retrieved results, and the *Pearson's product-moment* and *Spearman's rank* correlation coefficients $r$, $\rho$ of the retrieved results related to the most detailed assumptions $G_1$ as predicted outcome. Where $r$ denotes a linear correlation, $\rho$ is less sensitive to non-normality of distributions and enables to express the existence of a correlation between data arrays. Even for significant momentarily deviations, possible high correlation coefficients may denote that the retrieved data for most detailed data could be assessed based on a relationship of retrieved result with less-detailed data.

**Boundary conditions**

Occupancy behavior, domestic electricity consumption $P_{user}$ and solar irradiance $P_{sol}$ with different time resolutions $G$ are used as boundary conditions.

Due to the highly stochastic nature of domestic electricity consumption at building level, the impact of time resolution of user behavior mainly focuses on peak loads. As shown in fig.4 (upper,left), the overall occurrence of power loads above 2 $kW$ strongly differs. Whereas peak loads up to 8 $kW$ are observed for a 1-min time resolution $G_1$, the maximum power loads decrease down to 5 $kW$ for hourly data $G_{60}$. Although the main momentarily error $\Delta$ (upper,right) is found small due to the long periods of absence and standby powers which are unaffected by the time resolution, the errors on peak load are also most profound momentarily with extrema of 5 $kW$.

Similar analysis can be made for the solar irradiation (see fig.4 (lower)). The deviations on occurrence are found much smaller and are only found for the 10 % highest irradiations, but the momentarily error raises up to 0.4 $kW/m^2$ on days with variable weather conditions.

The depicted error on the extreme loads and the possible large momentarily error may be critical for control algorithms based on the net grid load De Coninck et al. (2010). Here, switching on or off the heat pump is decided based on threshold values of the power balance to improve grid stability by measures at building scale. Depending on the sensitivity of time resolution, the use of less detailed data may result in unreliable adjustments and conclusions resulting from control algorithms based on dynamic simulations.

**Thermal impact**

As shown in fig.5 (left), the influence of time resolution of boundary conditions on the thermal building response is small. Both annual thermal comfort and electricity consumption of the heat pump for SH and DHW shows little difference for different time frequencies.

The very high correlation coefficients and the small main deviation below 0.2°$C$ of the indoor operative temperature could be expected from the high thermal inertia of buildings. The small differences are caused by more stable temperature curves and less overshooting by overlapping internal gain peaks and heating gains for e.g. hourly data. The extrema up to 2.8°$C$ for the momentarily deviation of the operative temperature are caused by several reasons: $(i)$ shifts in time of the occupancy and thus in switch-on moments for SH, $(ii)$ sub-hourly heating patterns which disappear in low-frequency boundary conditions and $(iii)$ triggering (or not) of temperature-based control signals e.g. for opening of windows. The latter may be enforced by not taking into account the time constant of controllers in the simulations, whereas the first two reasons result from coupling the heating pattern to the stochastic occupancy profile.

Similar reasons cause large momentarily differences $\Delta$ in the heat pump power up to 3 $kW$. The large drop of the Pearson's product moment correlation coefficient $r$ down to 0.2 might suggest that the heating sequences of the residential building completely differ for the different time resolutions, whereas the

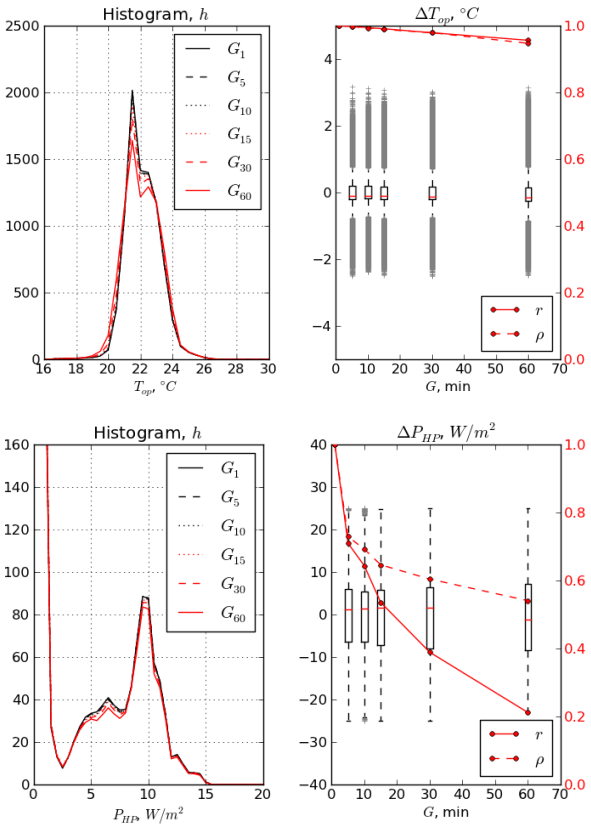


*Figure 5: (right) Deviations as Tukey-boxplot of the momentarily absolute error $\Delta$ in time and the Pearson's product-moment and Spearman's rank correlation coefficients $r$, $\rho$ for the different implemented time resolutions $G$ compared to the most-detailed resolution $G_1$ with 1-minute data, and (left) the overall density curve for the resulting indoor operative temperatures $T_{op}$ (upper) and the resulting heat pump power $P_{HP}$ (lower) for SH and DHW respectively.*

higher Spearman's rank correlation coefficient might suggest differently. Closer investigation of the heat pump power shows that the large extrema for momentarily deviations are caused by $(i)$ time shifts in the heat pump control signals due to deviations in the occupancy profile and $(ii)$ a variance in cycling of the heat pump when comfort is met as not all heating-up periods are equally long. The different switch-on and -off moments result in the rather high spread on the momentarily deviation as the heat pump power $P_{HP}$ changes during the heating cycle in each dwelling, whereas the very low correlation factors are caused by the large discontinuity of heat pump power pattern.

The depicted effects might not solely be assigned to time resolution as it is not the information source of a control algorithm but mainly its result. Within the simulations, required thermal comfort and SH control is coupled to the stochastic occupancy profile, whereas real-life heating patterns are defined by a combination of stochastic behavior and fixed daily household habits. Furthermore, current heating systems control may no longer apply for nZEBs due to reduced (system and) control efficiencies of hydronic systems for low heat demands .

**Electrical impact**

The sensitivity of the electrical impact towards time resolution is found to be more profound in contrast to the effect on thermal aspects. The reason is found in the very fast response time of electrical systems compared to thermal effects, but also in the responsiveness which is defined by both the sensitivity of domestic electricity consumption and local electricity generation, as well as the effect of the heat demand for SH and DHW by means of the electricity driven heat pump.

**Feeder loads and voltages**

As shown in fig.6 (upper, left), the main deviation on annual base of the net power exchange of a dwelling is mainly made on the net power demand side (denoted by negative values). The overall occurrence of power loads of 2 to 8 $kW$ strongly deviates and differs from the sensitivity of the boundary conditions as shown in fig.4 as it includes the electric power demand of the heat pump which coincides with local domestic demand. Although the main momentarily deviation $\Delta$ (upper, right) is small due to the long periods of absence unaffected by time resolution, the deviations on peak load are also found here most profound momentarily with extrema up to 9 $kW$. The high maximum deviation is due to the correlation between domestic electricity demands and heat demands at arrival.

A smaller deviation is noticed in the occurrence of a higher net supply (denoted by positive values in fig.6 (upper, left)) for 1-minute data compared to hourly data, whereas the maximum supply is found equal for all data.

More importantly, the resulting conclusion on the physical impact of this net power exchange can be found opposite as depicted for this net power exchange in fig.6 (lower). As shown in fig.6 (lower, left), the largest deviation is made on the over-voltage of the grid due to excessive BIPV generation and a resulting net supply. Here, hourly data $G_{60}$ result in an underestimation up to $9V$ on a maximum daily over-voltages of 18 $V$ compared to the feeder voltage for $G_1$, i.e. a relative deviation of factor 2. The strong underestimation resulting from the small deviation on the net power supply at building level is due to the strong correlation in time of net power supply at feeder level and a resulting strong accumulation of voltage increases. Contradictory to the large underestimation of peak power demands at building scale compared to 1-minute stochastic data $G_1$ (fig.6 (upper, left)), no lower extreme under-voltages are found for hourly simulations due to the stochastic nature and resulting weak coincidence in time of net power demand. As such, the depicted deviation on building scale will not result in underestimation of grid voltage drops.

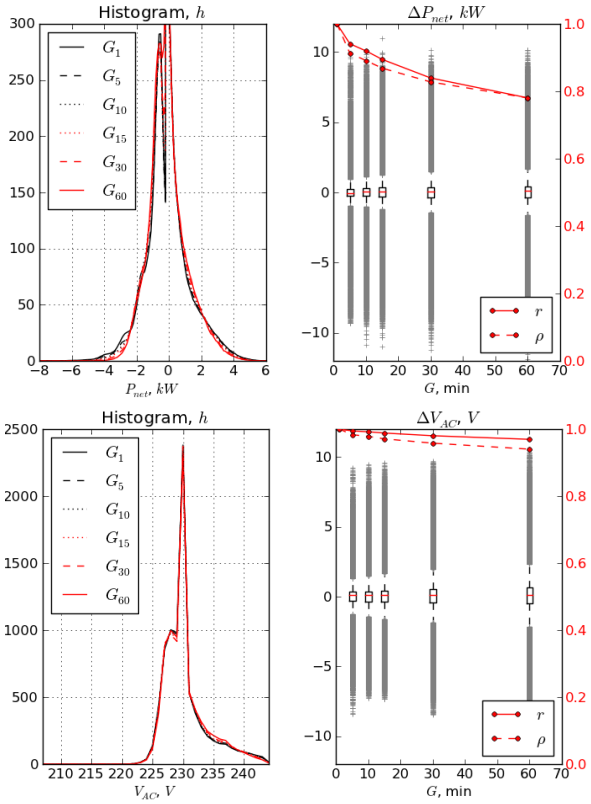


*Figure 6: (right) Deviations as Tukey-boxplot of the momentarily absolute error $\Delta$ in time and the Pearson's product-moment and Spearman's rank correlation coefficients $r$, $\rho$ for the different implemented time resolutions $G$ compared to the most-detailed resolution $G_1$ with 1-minute data, and (left) the overall density curvefor the net electrical power balance at building level $P_{net}$ (upper) and the distribution grid voltage $V_{AC}$ (lower) respectively. Negative values for $P_{net}$ depict a net demand, positive values a net supply to the feeder.*

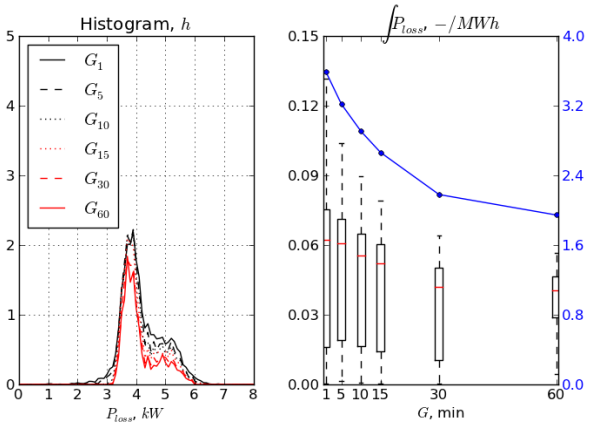


*Figure 7: The overall density curve for the resulting generation loss (left) and (right) the generation losses $\int P_{loss}$ per individual dwelling relative to its energy consumption and absolute in $MWh$ for the total neighborhood.*

### Generation losses

Within this case, the deviation caused by time resolution on the increased feeder voltages strongly influences the BIPV generation losses caused by BIPV curtailment (and vice versa) at the threshold voltage of 253 $V$ as shown in fig.7. The total annual generation loss at feeder level is found 3.6 MWh for $G_1$ where this value drops for larger time resolutions to 1.9 MWh for $G_{60}$ denoting a strong underestimation of 46% at feeder level. The total loss denotes 2.5% of the annual demand for $G_1$ and 1.4% for $G_{60}$.

With a one-minute time resolution $G_1$, 15 of the 33 dwellings in the neighborhood suffer from generation losses (depending on their location within the feeder topology) by BIPV curtailment, compared to 12 for $G_{60}$. The low number of dwellings indicate that the depicted error on the level of an individual dwelling will be larger than on feeder level. When only the dwellings which suffer from curtailment are assumed, the generation losses at level of an individual dwelling average 5.2% of the annual demand with a maximum of 13.1% for $G_1$ (see fig.7(right)), whereas lower values down to an average of 3.6% and a maximum of 5.6% for $G_{60}$ denoting an underestimation up to 57% at building level.

The found high errors on the generation losses are case-sensitive. For a over-dimensioned electricity feeder no generation losses will occur, whereas for an under-dimensioned feeder will suffer from large voltage fluctuations and excessive curtailment. These feeder designs will be assessed equally independent of the time resolution as a good or bad solution. The high deviations within this work are caused by the fact that the natural maximum of voltage fluctuation of the feeder are around the same value as the threshold value for BIPV curtailment.

## CONCLUSIONS

The sensitivity to time resolution of boundary conditions is studied for dynamic integrated simulation of thermal and electrical system of a residential neighborhood designed to be net zero-energy on annual basis. Variation of time resolution for domestic energy consumption and meteorological data shows the importance of sub-hourly data on electricity network investigation, but its usage should always be weighted against less detailed data with respect to CPU time, availability and representativeness.

Large simultaneity of net power supply at building level in the residential built environment results in strong underestimation of grid over-voltages for hourly irradiance data. The use of minutely meteorological data is critical for assessment of power losses due to inverter switch-offs caused by grid voltage increases. On the demand side, the main deviation is found in a possible correlation of heat pump power demands for SH or DHW but not in the stochastic nature of domestic electricity consumption. Here, sub-hourly

demand profiles are less critical if they are not used in grid balancing control strategies.

The depicted error on the extreme loads and the possible large momentarily error may be critical for control algorithms based on the net grid load. Depending on the sensitivity of time resolution, the use of less detailed data may result in unreliable adjustments and conclusions resulting from control algorithms based on dynamic simulations. With respect to this, it must be noted that the high sensitivity of the electric feeder and its resulting losses may not be generalized. They depend on the strength of the electric feeder, the feeder load (which concerns only a residential load within this work) and the set boundary limits with respect to the natural fluctuations of the feeder.

## ACKNOWLEDGEMENTS

The authors gratefully acknowledge the K.U.Leuven Energy Institute (EI) for funding this research through granting the project entitled *Optimal energy networks for buildings*.

## REFERENCES

Baetens, R. and Saelens, D. 2011. Integrating occupant behaviour in the simulation of coupled electric and thermal systems in buildings. In *8th Int. Modelica Conf.*, March 20-22, Dresden.

Becker, B. R. and Stogsdill, K. E. 1990. Development of Hot Water Use Data Base. In *ASHRAE Transactions*, volume 96, pages 422–427, Atlanta, GA. American Society of Heating, Refrigerating and Air Conditioning Engineers.

Daikin Europe N.V. 2006. Technical data Altherma ERYQ007A, EKHB007A / EXHBX007A, EKSWW150-300. Technical report.

De Coninck, R., Baetens, R., Vebruggen, B., Driesen, J., Saelens, D., and Helsen, L. 2010. Modelling and simulation of a grid connected photovoltaic heat pump system with thermal energy storage using Modelica. In *8th Int. Conf. on System Simulation in Buildings*, page P177.

EN 12831 2003. *Heating systems in buildings - Method for calculation of the design heat load*.

EN 442-2 1996. *Radiators and convectors - Part 2: Test methods and rating*.

European Commission 2010. SEC(2011) 463 final - Smart Grids: from innovation to deployment, COM(2011)202 final.

Fairey, P. and Parker, D. 2004. A Review of Hot Water Draw Profiles Used in Performance Analysis of Residential Domestic Hot Water Systems. Technical report, Florida Solar Energy Center, Florida.

FOD Economie 2008. Bevolking - Private, grootte en collectieve huishoudens. Technical report.

Heiple, S. and Sailor, D. J. 2008. Using building energy simulation and geospatial modeling techniques to determine high resolution building sector energy consumption profiles. *Energy and Buildings*, 40:1426–1436.

IEC 60364-6 2006. *Low-voltage electrical installations - Part 6: Verification*.

Maes, D. 2005. http://wwwa.vito.be/edisontest/qs/index.asp.

Meteotest 2008. METEONORM Version 6.1 - Edition 2009.

Richardson, I., Thomson, M., Infield, D., and Clifford, C. 2010. Domestic electricity use: A high-resolution energy demand model. *Energy and Buildings*, 42(10):1878–1887.

Robinson, D., Campbell, N., Gaiser, W., Kabel, K., Lemouel, A., Morel, N., Page, J., Stankovic, S., and Stone, A. 2007. SUNtool A new modelling paradigm for simulating and optimising urban sustainability. *Solar Energy*, 81(9):1196–1211.

Tanimoto, J., Hagishima, A., and Sagara, H. 2008. Validation of methodology for utility demand prediction considering actual variations in inhabitant behaviour schedules. *Journal of Building Performance Simulation*, 1(1):31–42.

The European Parliament 2010. Directive 2010/31/EU of the European Parliament and of the Council of 19 May 2010 on the nergy performance of buildings (recast).

The Institute of Electrical and Electronics Engineers 2010. IEEE 34 Node Test Feeder. Technical report.

Vanneste, D., De Decker, P., and Laureyssen, I. 2001. Sociaal-Economische Enquête 2001. Monografie. Woning en woonomgeving in België. Technical report.

Verbruggen, B., Van Roy, J., De Coninck, R., Baetens, R., Helsen, L., and Driesen, J. 2011. Object-oriented electrical grid and photovoltaic system modelling in Modelica. In *8th Int. Modelica Conf.*, March 20-22, Dresden.

Widén, J. 2009. *Distributed Photovoltaics in the Swedish Energy System*. PhD thesis.

Yamaguchi, Y. and Shimoda, Y. 2010. District-scale simulation for multi-purpose evaluation of urban energy systems. *Journal of Building Performance Simulation*, 3(4):289–305.